Description of Mathematical Model

This document has the details of the mathematical model used for the simulations that are discussed in the manuscript titled "Hemoglobinopathies affect the intraerythrocytic multiplication of *P. falciparum,"* by Svetlana Glushakova, Amanda Balaban, Philip G. McQueen, Rosane Coutinho, Jeffery L. Miller, Ralph Nossal, Rick M. Fairhurst, and Joshua Zimmerberg. The reference numbering in this supplement is independent of that in the main text. Also in this supplement, Table 1 refers to a table at the end of this document, and not to the Table 1 in the main text.

Introduction

We state here a theoretical model of the population growth of within-host malaria parasites which are exposed to a pyrogenic innate response. The model is based on ideas from theoretical ecology describing a population of individual organisms that age at different rates [1, 2], and is similar to ones previously used by one of the authors (PGM) in theoretical population studies of malaria infections [3-5]. The discussion here follows that in [4] closely, but with some changes in notation.

Consider a population of individuals that age while progressing to the next stage of life development or senescence. Not all individuals take the same amount of time to age, and the youngest members of the population might be created at a time-varying rate s. This is a time delay system which can be difficult to solve, so we here introduce a set of coupled ordinary different equations (ODEs) that govern the time evolution of a set of fictitious variables, P_1 , P_2 , P_3 , . . . P_N; the sum of which is the total population. The ODEs are chosen so that the rate at which individuals leave the population for the next stage (or death) is approximately a normal function of time t with mean duration D and variance $\sigma^2 = D^2N^{-1}$. Ignoring environmental influences which might cull the population, the ODEs are

$$P_1' = s(t) - \Lambda P_1 \text{ (where } \Lambda = ND^{-1})$$

$$P_n' = \Lambda(P_{n-1} - P_n),\ 1<n\leq N. \qquad (1)$$

In this formalism, the quantities D and σ determine N, the total number of components. Thus measureable quantities set the properties of the abstract ODE system. (Note that if $D = \sigma$, this system of equations reduces to a single equation describing exponential decay--see details of implementation below.) All population sizes are stated as number per μL of blood. Our model is adjusted to fit the natural history of *Plasmodium falciparum*

Model: Reproductive Rate of the Parasite

A measurable quantity that constrains the model parameters is the initial reproduction rate of a parasite, $\mathbf{R_0}$, defined as the average number of descendants an individual parasite would have at the beginning of bloodstream infection in the absence of any host response to the parasite. If $T_{D\mathrm{m}}$ (duration of the merozoite stage) is much less than the duration of the infected RBC stage, then [3],

$$\mathbf{R_0} = IMF\, \zeta V_0\, T_{Dm} (\, 1 + \zeta\, V_0\, T_{Dm})^{-1} \qquad \text{(Eq. 2)}$$

Here V_0 is the initial density of the RBC population vulnerable to the parasite species, ζ is the binding affinity of merozoites to RBCs, and *IMF* is the average number of merozoites released per bursting schizont. (For *P. falciparum*, V_0 = normal basal RBC count = $5x10^6 ml^{-1}$.) Experimental evidence suggests that T_{Dm} is several minutes; we take it as 0.1hr [6]. For this study, we take *IMF* to be either 22 or 26, and we choose ζ so that $\mathbf{R_0}$ is 0.9375 times the corresponding value of *IMF*. (A study of the efficiency of invasion of merozoites of the 3D7 strain of *P. falciparum* suggests that $\mathbf{R_0}$ is 90-100% in many malaria patients. [7])

Model: Parasite Population Dynamics

Let T_{DI} be the average duration of the infected RBC stage, with standard deviation s_{IBC}. Then $N_{cI} = T_{DI}^2/\sigma_{IBC}$. is the number of compartments needed to described the IBC development. Let I_n be number of infected RBCs per μl in compartment n. We assume that the intracellular parasites are being attacked by an immune response, e.g., via their modification of the RBC membrane, that removes them at a rate χ, which has its own dynamics. Then

$$dI_1/dt = \zeta\mu\, E_T - (k_I + \chi)\, I_1$$

$$dI_n/dt = k_I\, I_{n-1} - (k_I + \chi)\, I_n, \quad 1 < n < N_{cI} + 1 \qquad \text{(Eq.3)}$$

Here $k_I = N_{cI}/T_{DI}$ plays a role similar to that of Λ in Eq. 1 , μ is the merozoite density, ζ is the binding affinity between the merozoites and vulnerable RBCs, and E_T is the total uninfected RBC count. We took T_{DI} = 48hr [8]. For each immune and erythropoietic response, we evaluated the behavior of the model for several values of σ_{IBC} (given in Table 1). The discussion after Equation 2 gives the details on how the value of ζ is set.

We use just one compartment for the merozoite stage, due to its short survival time in the blood, $T_{Dm} = \sigma_m$ = 0.1hr [6]:

$$d\mu/dt = IMF\, k_I I_{NcI} - \mu(\, \zeta\, E_T + 1/T_{Dm}\,) + L(t) \qquad \text{(Eq. 4)}$$

where the first term on the r.h.s. of this equation represents the release of merozoites from infected rbc's, and $L(t)$ is the infusion of primary merozoites of the given species from the liver into blood, a process that apparently releases10^4 - 10^5 merozoites within a hours [9]. In our simulations, the initial time (t = 0) corresponds to the release of the first parasite from the liver. For simplicity, we took $L(t)$ to be a constant for the first 12 hours such that a total of 0.002 μl^{-1} is released, (corresponding to a release of 10^4 primary merozoites into a blood volume of $5x10^6\mu l$), and then zero afterwards.

In *P. falciparum* malaria, the intraerythrocyte parasites sequester onto blood vessel walls during the second phase (last 24 hours) of intraerythrocyte development. Sequestered parasites can

readily release large numbers of merozoites that attack neighboring RBCs [10]. Thus, in our model we consider the IBC compartments to include sequestered as well as freely-circulating infected red blood cells.

Model: Erythrocyte Population Dynamics

The RBC development chain is divided into three parts. The dynamics of the youngest erythrocytes, the reticulocytes, is described by

$$dR_1/dt = ES(t) - k_R R_1 - \zeta\mu R_1$$

$$dR_n/dt = k_R (R_{n-1} - R_n) - \zeta\mu R_n, \quad 1 < n < N_{cR} + 1 \qquad \text{(Eq. 5)}$$

Correspondingly, we write for mature red blood cells:

$$dM_1/dt = k_R R_{NcR} - k_M M_1 - \zeta\mu M_1$$

$$dM_n/dt = k_M (M_{n-1} - M_n) - \zeta\mu M_n, \quad 1 < n < N_{cM} + 1 \qquad \text{(Eq. 6)}$$

and for senescent red blood cells:

$$dS_1/dt = k_M M_{NcM} - k_S S_1 - \zeta\mu S_1$$

$$dS_n/dt = k_S (S_{n-1} - S_n) - \zeta\mu S_n, \quad 1 < n < N_{cS} + 1 \qquad \text{(Eq. 7)}$$

(We separate the senescent stage from the mature stage to allow for possible models of *P. malariae* infections in which mainly senescent erythrocytes are attacked.) Here, $k_R = N_{cR}/T_{DR}$, $k_M = N_{cM}/T_{DM}$, and $k_S = N_{cS}/T_{DS}$, where the T_{DR}, T_{DM}, and T_{DS} are the durations of the respective red blood cell stages, and N_{cR}, N_{cM}, and N_{cS} are the respective numbers of compartments used for each stage (as set by Eq. 2 above). ES(t) is the rate of new RBC production at time t. Based on physiologically reasonable values [11], we took T_{DR} = 36 hr with σ = 6 hr, T_{DM} = 2796 hr with σ = 168 hr, and T_{DS} = 48hr with σ = 12 hr. The total uninfected red blood cell count, E_T, is equal to the sum of all the R, M, and S compartments. If E_T drops below $3x10^6$ μl^{-1} (i.e. 0.6 x the basal count of a typical healthy adult), then we assume that the host dies of catastrophic anemia. Studies of RBC or hemoglobin levels in patients with *P. falciparum* infections suggest that the red blood cell count can collapse to similarly low fractions of the basal count [12, 13].

Model: Erythropoietic Response

The dynamics for the marrow RBC source depend on the host response to losses of uninfected RBCs. Let $\Phi = ES_0 - dE_T/dt - \delta\zeta\mu E_T$, where ES_0 is the basal rate of RBC production (which maintains a healthy basal count of $5x10^6 \mu l^{-1}$), and ζ and μ are as indicated above in equations 3 and 4. The use of the factor δ is a simplistic way to account for the dyserythropoietic effects during infection. [14] We model the dynamics of ES(t) with the following ODE:

$$dES/dt = \lambda_{ES}\,(\Phi - ES(t)), \qquad ES_{MN} < \Phi < ES_{MX}$$

$$= \lambda_{ES}(ES_{MX} - ES(t)),\ \Phi > ES_{MX}$$

$$= \lambda_{ES}(ES_{MN} - ES(t)),\ \Phi < ES_{MN} \qquad \text{(Eq. 8)}$$

ES_{MX} is the maximum RBC production rate, and $1/\lambda_{ES}$ is a response time to changes in the rate of RBC loss. For a healthy compensatory response to RBC loss [11], $ES_{MX}/ES_0 = 5$ and $1/\lambda_{ES} =$ 48hr. ES_{MN} is a minimum production rate; with dyserythropoiesis, the RBC production rate would be driven to ES_{MN}. The parameter δ was varied between 0 and 10; (see Table 1).

Model: Immune Response Dynamics

We considered the pyrogenic innate response often observed in malaria: fast-activating but short-acting [5, 15]. We assumed that this response is triggered when the merozoite level exceeds a threshold density *Th*, producing an actuator component *A*. The actuator in turn produces an attacker that removes the intracellular parasites at a rate χ. The whole response is self-limiting so that χ does not exceed a maximum value χ_{Max}. The dynamics are described by

$$dA/dt = FB_A\, FB_K\, (\,\Theta(\mu - Th) - \lambda_A\, A_0) - \lambda_A\, A$$

$$d\chi/dt = FB_K\ \lambda_{\chi}\,(A - A_0) - \lambda_{\chi}\, A \qquad \text{(Eq. 9)}$$

where $\Theta(x) = x$ if $x > 0$, zero otherwise, and

$$FB_A = (\,1 - (\,A - A_0)\,\Delta\, A_{Max}^{-1}\,)\ \ \Theta(\Delta A_{Max} - A + A_0)$$

$$FB_K = (\,1 - \chi\,\chi_{Max}^{-1})\ \ \Theta(\chi_{Max} - \chi)$$

The self-amplication parameter *a* is set to 10, and the background actuator level A_0 is set to $0.1\mu l^{-1}$. The *FB* factors enforce self-limiting feedback. The parameter ΔA_{Max} limits the growth of the actuator and is set to $10\mu l^{-1}$. We took $1/\lambda_A = 1$ hr, and $1/\lambda_{\chi} = 2$ hr. This model innate response emulates the cytokine dynamics reported in malaria patients for the chosen values for a, A_0, λ_A, and λ_{χ}. [5, 15] Parameters *Th* and are χ_{Max} varied from simulation to simulation; see Table 1. The range of values indicated in Table 1 for *Th* and are χ_{Max} is the range found to encompass the magnitude and time series of parasitemia that is seen in neurosyphilis patients with *Plasmodium falciparum* [16].

Sampling the parameter space

The values of several model parameters were varied from simulation to simulation, either

because the parameters vary strongly from patient to patient, or their values are not known. Table 1 lists all these parameters, and the range of plausible values from which the values for simulation were chosen. For a given value of number of merozoites released per bursting schizont, p, the Latin hypercube algorithm [17] was used to sample among the relevant parameters in the following manner. Let p1, p2, . . . pM be the parameters varied for given model class and divide the plausible range for each pn into ten equal intervals. We define a $10 \times M$ matrix M, the columns of which consist of a random ordering of the integers 1 through 10, with no integer repeated in a column. The integers are associated with the parameter intervals as follows: integer k = Mi,n labels interval k for parameter pn. The first simulation uses values of p1, p2, . . . pM chosen randomly within the intervals labeled by M1,1, M1,2, . . . M1,M. The second simulation uses values chosen randomly within the intervals labeled by M2,1, M2,2, . . . M2,M. This procedure is repeated until values in the intervals labeled by M10,1, M10,2, . . . M10,M are used. The order of the integers in each column are scrambled to repeat the procedure again. Thus, for a given p, we used 1000 randomized version of M so that there would be a total of 10000 simulations. We used the Latin hypercube algorithm to attempt uniform sampling of the parameter space for a class of models, although with so many variable parameters the sampling will not be perfect.

Model: Simulation Strategy

The system of ordinary differential equations was solved using the fifth-order Runge-Kutta-Fehlberg algorithm with adaptive stepsize control for time integration, [18, 19] so that the difference between the fourth- and fifth-order solutions for each component of the system was less than one part in 10^6.

If at any point either (1) the merozoite count, (2) the total infected red blood cell count, or (3) the total uninfected RBC count E_T fell below 1 in a total blood volume of 5×10^6ml, the values of all compartments that contributed to that particular count were reset to zero. As stated above, the simulation stopped if E_T dropped to under $3 \times 10^6 \mu l^{-1}$.

References for This Supplement

1. Lloyd AL (2001) The dependence of viral parameter estimates on the assumed viral life cycle: limitations of studies of viral load data. Proc Roy London Soc Ser B 268: 847-854.

2. Lloyd AL (2001) Destabilization of epidemic models with the inclusion of realistic distributions of infectious periods. Proc Roy London Soc Ser B 268: 985-993.

3. McQueen PG, and McKenzie FE (2004) Age-structured red blood cell susptibility and the dynamics of malaria infections, Proc Natl Acad Sci USA 101: 9161-9166.

4. McQueen P, McKenzie F (2008) Host control of malaria infections: constraints on immune and erythropoeitic response kinetics. PLoS Comp Biol 2008, 4:e100149.

5. McQueen P: Population dynamics of a pathogen: the conundrum of vivax malaria. Biophys Rev 2010, 2:111–120.

6. Johnson JG, Epstein N, Shiroishi T, and Miller LH (1980) Factors affecting the ability of isolated *Plasmodium knowlesi* merozoites to attach to and invade erythrocytes. Parasitology 80: 539-550.

7. Lawrence G, Cheng Q, Reed C, Taylor D, Stowers A, Cloonan N, Rzepczyk C, Smillie A, Anderson K, Pombo D, Allworth A, Eisen D, Anders R, and Saul A. (2000) Effect of vaccination with 3 recombinant asexual-stage malaria antigens on initial growth rates of *Plasmodium falciparum* in non-immune volunteers. Vaccine 18:1925-1931

8. White NJ, Breman JG (2001) Malaria and babesiosis. In: Braunwald E, Fauci AS, Isslbachter JK, Kasper DL, Hauser SL, Longo DI, Jameson JL eds., Harrison's Principles of Internal Medicine. New York: McGraw-Hill, pp. 1203-1213.

9. Baer K, Klotz C, Kappe SHI, Schneider T, and Frevert U (2007) Release of Hepatic *Plasmodium yoelii* Merozoites into the Pulmonary Microvasculature. PLoS Pathog 3:1651-1668.

10. Glushakova S, Yin D, Li T, and Zimmerberg J (2005) Membrane transformation during malaria parasite release from human red blood cells. Curr Biol 15: R760-R761.

11. Rapaport, S.I. (1987) Introduction to Hematology. Philadelphia: J. B. Lippincott. 624p.

12. Srichaikul T, Siriasawakul T, and Poshyachinda M (1976) Ferrokinetics in patients with malaria: haemoglobin synthesis and normoblasts in vitro. Trans R Soc Trop Med Hyg 70: 244-246.

13. Awandare GA, Ouma Y, Ouma C, Were T, Otieno R, Keller CC, Davenport GC, Hittner JB, Vulule J, Ferrell F, Ong'echa JM, and Perkins DJ (2007) Role of monocyte-acquired Hemozoin in suppression of macrophage Migration Inhibitory Factor in children with severe malarial anemia. Infect Immun 75: 201-210.

14. Wickramasinghe SN and Abdall SH (2000) Blood and bone marrow changes in malaria. Balliere's Clin Haematol 13: 277-299.

15. Karunaweera ND, Grau GE, Gamage P, Carter R, and Mendis KN (1992) Dynamics of fever and serum levels of tumor necrosis factor are closely associated during clinical paraoxysms in *Plasmodium vivax* malaria. Proc. Natl. Acad. Sci. USA 89: 3200-3203.

16. Simpson JA, Aarons L, Collins WE, Jeffery GM, White NJ (2002) Population dynamics of untreated *Plasmodium falciparum* malaria within the adult human host during the expansion phase of the infection. Parasitology 124: 247-263.

17. McKay M, Beckman R, Conover W (1979) A comparison of three methods for selecting values of input variables in the analysis of output from a computer code. Technometrics 1979, 21:239-245.

18. Press WH, Teukolsky SA, Vettering WT, Flannery BP (1992) Numerical Recipes in C. Cambridge UK: Cambridge University Press.

19. Cash JR, and Karp AH (1990) A variable order Runge-Kutta method for initial-value problems with rapidly varying right-hand sides. ACM Trans Math Soft 16: 201-222.

Table 1: Values of Parameters Varied from Simulation to Simulation

Parameter	Equation where used	Range in values
δ	8	0 - 10
$\text{Log}(\sigma_{IBC} \times hr^{-1})$	3	Log(0.3)- Log(5.9)
Log(Th x μl)	9	$\text{Log}(10^{-5}) - \text{Log}(10)$
$\text{Log}(\chi_{Max} \times hr)$	9	Log(0.05) – Log(50)

Supplementary Material

Figure S1. Predicted effect of intraerythrocytic multiplication factor (IMF) on the onset of detectable parasite densities by thick blood smear examination. (**A**) The fraction of simulations for which Max_{IBC} exceeds the threshold of detectable parasite density (10/μL) in routine thick blood smear examination, in different parts of the immune-parameter space at 6 and 10 days after primary release. The 10,000 simulations done for each IMF value are binned by their values of threshold density of merozoites that trigger the response, *Th*, and maximum killing rate of infected erythrocytes, χ_{Max}. The horizontal extent of the blocks shows the bin size *Th,* and the vertical extent shows the bin size χ_{Max}. The gray-scale code used to specify the fraction values is shown in the inset.

Table S1. Representative hematological parameters from subjects with hemoglobinopathies.

Figure S1

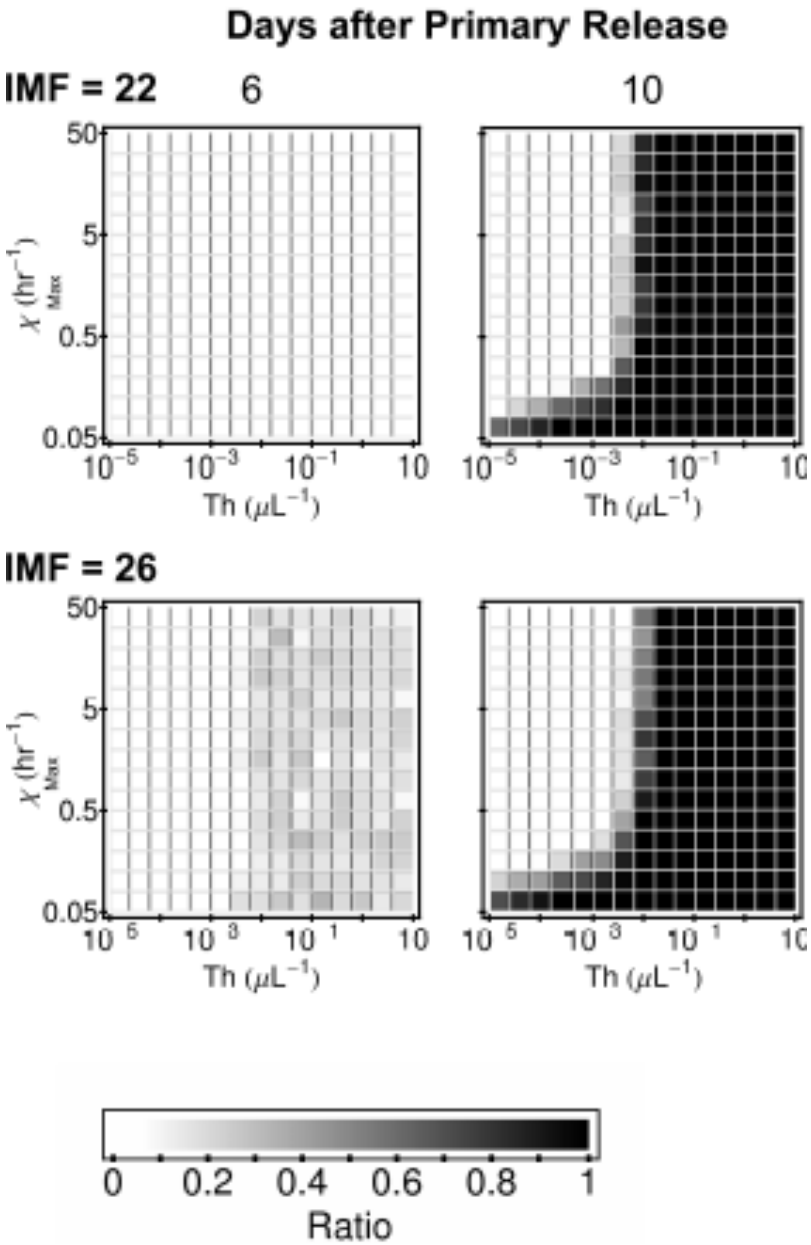
Days after Primary Release
IMF = 22
6
10
50
5
0.5
0.05
χ (hr^{-1}) Max
10^{-5} 10^{-3} 10^{-1} 10
Th (μL^{-1})
IMF = 26
0 0.2 0.4 0.6 0.8 1
Ratio

SUPPLEMENTAL TABLE 1. REPRESENTATIVE HEMATOLOGICAL PARAMETERS FROM SUBJECTS WITH HEMOGLOBINOPATHIES

Subject	WBC	RBC	HGB	HCT	MCV	MCH	MCHC	RDW	Platelet count
	K/µL	M/µL	g/dL	%	fL	pg	g/dL	%	K/µL
#1, HbSS	5.43	2.63 (L)	10.8 (L)	30.5 (L)	116.0 (H)	41.1 (H)	35.4	17.5 (H)	295
#2, HbSS	5.83	1.98 (L)	9.0 (L)	25.9 (L)	129.9 (H)*	45.0 (H)*	34.6*	15.2 (H)	348
#3, HbAS	9.48	4.27	12.2	35.7	83.6	28.6	34.2	13.5	307
#4, HbAS	6	4.6 (L)	13.4 (L)	39.6 (L)	86.1	29.1	33.8	12.2	179
#5, HbAS	3.48 (L)	4.47	13.3	38.5	86.1	29.8	34.5	13.6	236
#6, α-Thal trait (αα/α-)	5.01	5.54	14.2	44.1	79.6	25.6 (L)	32.2 (L)	15.9 (H)	232
#7, α-Thal trait (α-/α-)	6.29	5.97	13.1 (L)	42.1	71.2 (L)*	22 (L)*	30.9 (L)*	15.5 (H)	217
#8, α-Thal trait (α-/α-)	8.66	6.48 (H)	14.1	44.8	69.1 (L)	21.8 (L)	31.5 (L)	15.4 (H)	223
#9, β-Thal trait	4.68	4.98	11.8	36.6	73.5 (L)	23.7 (L)	32.2 (L)	15.0 (H)	207
#10, β-Thal trait	7.39	5.65 (H)	12.1	37.4	66.2 (L)	21.4 (L)	32.4	14.7 (H)	232
#11, β-Thal trait	7.52	4.56	10.2 (L)	32.6 (L)	71.5 (L)	22.4 (L)	31.3 (L)	14.2	240
#12, β-Thal trait	6.27	6.66 (H)	14.1	43.5	65.3 (L)	21.2 (L)	32.4	15.5 (H)	213

LOW (L)	HIGH (H)

*** Mean values from several blood samples**